Journal of Inorganic and Organometallic Polymers and Materials (2022) 32:2928–2939
https://doi.org/10.1007/s10904-022-02318-9

Facile Synthesis of Ferrocene-Based Polyamides and Their Organic Analogues Terpolyamides: Influence of Aliphatic and Aromatic Sequences on Physico-Chemical Characteristics

Tehmina Khan[1] · Zareen Akhter[1] · Asghari Gul[2] · Arshad Saleem Bhatti[3] · Adeela Rehman[1,4,5]

Received: 4 February 2022 / Accepted: 21 March 2022 / Published online: 9 April 2022

Abstract
Efforts have been devoted to synthesize and characterize processable polymers with desired properties. Herein, four different series of aromatic and aliphatic terpolyamides were prepared via solution phase polycondensation of 4,4′-oxydianiline and hexamethylenediamine (HMDA) with various diacids chlorides (isophthalyol dichloride, terepthalyol dichloride, 1, 1′-ferrocene dicarboxylic acid chloride and trans-azobenzene-4, 4′-dicarbonyl chloride). The structural, morphological and physico-chemical nature of as prepared polymers was explored by Fourier-transform infrared spectroscopy, scanning electron microscopy, thermal analysis (TGA and DSC), and wide-angle x-ray diffraction. Moreover, an aliphatic diamine was incorporated in varying concentration as a flexible methylene spacer and the effect of its concentration on the properties of polyamides was also studied. Changes in various physico-chemical properties such as solubility, inherent viscosity, surface morphology and flame retarding behaviour were investigated. Marked difference in morphology and solubility was observed with the change in the ratio of segments in the chain. Inherent viscosities of polymers ranged from 1.8052–1.6274 dl/g indicating reasonably moderate molecular weights. Interestingly, ferrocene based aromatic polymers were more thermally stable (T_g 260 °C, T_i 310 °C, T_h 525 °C, T_f 720 °C, for PF_0), and also found to exhibit best flame retarding behavior (limiting oxygen index value for $PF_0$is LOI 33.15%).

Keywords Ferrocene based polyamides · Terpolyamides · Thermal behavior · Limiting oxygen index · Viscosity measurement

1 Introduction

Polyamides continue to be one of the most promising class of polymers by virtue of their remarkable high temperature thermo-mechanical properties [1, 2]. High temperature tolerance along with distinctive and versatile properties of polyamides has earned these thermoplastics a place among the high-performance engineering plastics. The characteristic features associated with each class of polyamides are conferred due to their variable structural aspects of the monomers. Aramids have rigid phenyl rings that impart stiffness to the polymer chain and dramatically increase the thermo-mechanical properties, abrasion resistance, chemical resistance, solvent resistance, and impart better properties like higher impact strength, low coefficient of thermal expansion comparable to the high-performance materials [3, 4]. However, the polymer processing via melt technique is difficult in aramids attributed to the formation of highly viscous melts. On contrary, Nylons, having aliphatic monomers, are

✉ Zareen Akhter
zareenakhter@yahoo.com

✉ Adeela Rehman
adeelarehman00@gmail.com

1 Department of Chemistry, Quaid-i-Azam University, Islamabad 45320, Pakistan

2 Department of Chemistry, COMSATS IIT, Islamabad, Pakistan

3 Department of Physics, COMSATS IIT, Islamabad, Pakistan

4 Department of Mechanical Engineering, College of Engineering, Kyung Hee University, Yongin 446-701, Republic of Korea

5 Department of Chemistry, Inha University, 100 Inharo, Incheon 22212, Korea

silky materials that offer better chemical resistance, weathering properties, resilience and excellent abrasion resistance, though their thermo-mechanical properties are inferior to those of aramids. To circumvent the thermo-mechanical problems, incorporation of the metal ions into polymers has given a new dimension to the polymer science. This task has been eased by the synthesis of ferrocene-based polymers. This not only introduces the strong and stable iron as the metal center but also imparts firmness to the chains and characteristics associated to ferrocene such as flame retarding behavior, electroactivity, redox properties etc. [5, 6]. Ferrocene has proved to enhance the features of the polymers to a great extent and has made them a profitable choice where materials are expected to show superior electroactivity, conductance and semi-conductance, catalytic activity, optical properties, thermo-mechanical stability, magnetism and flame-retarding behavior [7–9].

Recently, the properties of the polyamides are optimized by terpolymerization/copolymerization with other materials such as flexible spacers having their distinguishing features thereby incorporating the properties of both polyamides and the induced material with desirable features [10–12]. Consequently, the processibility of material is made easier without compromising over the loss of distinguishing features like stability and thermo-mechanical strength. Herein, the notion behind this effort was to investigate the effect of subsequent increase of a flexible spacer on certain physicochemical properties of polyamides. This task was achieved by introducing a six-membered methylene chain in various concentrations so as to observe the modifications generated in the properties and the ease in melt processing. Our work is based on the investigation of aliphatic, aromatic, and organometallic based polyamides and their physicochemical studies. In this study, new monomers were synthesized, and the functional groups were incorporated in the polymer chains to delineate their effect on the properties of polymers. The study is important as polyamides have a wide range of applications in daily life [13]. Based upon their intriguing properties such as thermal stability and thermal retardant behavior, they could be explored for further potential applications.

2 Experimental Procedures

2.1 Materials

Ferrocene (m.p = 173 °C), triethylamine (TEA, b.p = 89 °C), 4-nitrobenzoic acid (m.p = 236 °C), acetyl chloride (b.p = 50 °C), 4, 4'-oxydianiline (m.p = 191 °C) and aluminium chloride (m.p = 194 °C), were purchased from Fluka (Switzerland) and used as such whereas isophthaloyl chloride (IPC) (m.p = 42 °C) and terepthaloyl chloride (TPC) (m.p = 83 °C) were purchased from Aldrich (Germany). Potassium carbonate (anhydrous) (m.p = 890 °C), sodium hydroxide (m.p = 392 °C) and thionyl chloride were obtained from Merck (Germany). Commercially available sodium hypochlorite solution was used having 12–15% strength per liter. 1,6-hexanediamine (60% aqueous solution, b.p = 204 °C) was purchased from Acros Organics (New Jersey, USA). All solvents used were purchased from Merck (Germany) whereas tetrahydrofuran (THF) was purchased from Riedel de Haën and dimethylsulfoxide (DMSO) was obtained from Fluka (Switzerland). All the solvents were dried and distilled before usage.

2.2 Synthesis of Monomers

2.2.1 Synthesis of 1, 1′-Ferrocenedicarboxylic Acid Chloride (FcDC)

Synthesis of 1,1′-ferrocenedicarboxylic acid chloride is carried out via three-step procedure which involves synthesis of 1, 1′-diacetyl ferrocene followed by conversion into 1,1′-ferrocene dicarboxylic acid and finally to 1,1′-ferrocene dicarboxylic acid chloride [14–16].

2.2.2 Synthesis of Trans-azobenzene-4, 4′-Dicarbonyl Chloride (TADC)

Synthesis of trans-azobenzene-4,4′-dicarbonyl chloride (TADC) involved two steps comprising preparation of trans-azobenzene-4,4′-dicarboxylic acid followed by the conversion into acid chloride by the procedure as shown in Scheme 1 [16].

2.3 Synthesis of Polymers

All the organic and ferrocene-based polymers are synthesized by Scheme 2. The pre-weighed mixture of aromatic and aliphatic diamines with various compositions (net quantity 1.88 mmol) were dissolved in 20 mL of dried THF in a pre-baked, two-necked, 250 mL round bottom flask equipped with a magnetic stirrer and a condenser. The reaction mixture was stirred for 15 min and then 10 mL of triethylamine (TEA) was added to the flask at 0 °C which was maintained by ice bath. After stirring for 20 min, dicarbonyl chloride (1.92 mmol) solution (in dried THF) was added drop wise to the flask with vigorous stirring. Temperature of the reaction mixture was raised slowly to the room temperature. After stirring for 5–6 h, the reaction mixture was refluxed for 1 h. The precipitated product was filtered, washed sequentially with THF and methanol to remove unreacted precursors and side products. The finally obtained polymer material was dried in vacuum for 24 h.

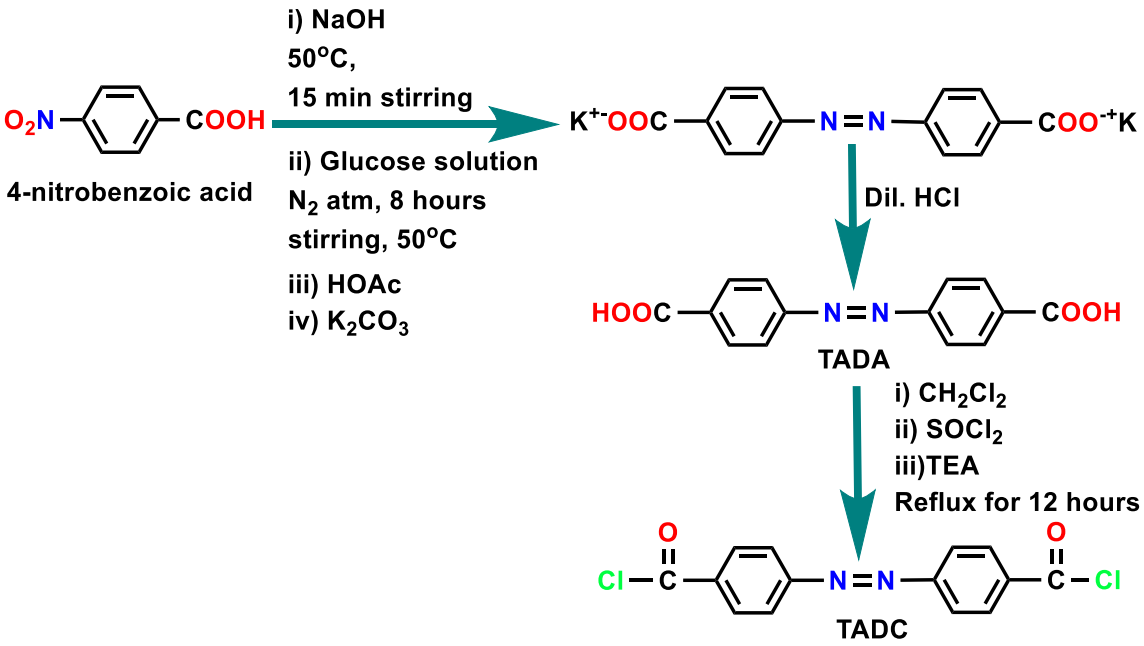

Scheme 1 Synthesis of trans-azobenzene-4, 4′-dicarbonyl chloride (TADC)

2.3.1 Synthesis of PF Series

i. PF_0
Aliphatic diamine 0%, Aromatic diamine 100% (1.88 mmol), Color: Brown. Yield: 84%. FT-IR (in cm^{-1}): 3333.9 (N–H), 3157 (Ar–H), 1637.2(C=O), 1601.4 (N–H), 1312.6 (C–N), 1099.5 (C–O–C), 498.2 (Fe-Cp).

ii. PF_{50}
Aliphatic diamine 50% (0.94 mmol), Aromatic 50% (0.94 mmol), Color: Dark brown. Yield: 78%. FT-IR (in cm^{-1}): 3448.4–3284.9 (N–H), 3110–3082 (Ar–H), 2944.9 (CH_2), 1634.2 (C=O), 1519.9 (N–H), 1273.3 (C–N), 1065.4 (C–O–C), 492.1 (Fe-Cp).

iii. PF_{70}
Aliphatic diamine 70% (1.316 mmol), Aromatic 30% (0.564 mmol), Color: Dark brown. Yield: 90%. FT-IR (in cm^{-1}): 3273.6 (N–H), 3167.8 (Ar–H), 2930.1 (CH_2), 1622.3 (C=O), 1531.6 (N–H), 1341.3 (C–N), 1026.4 (C–O–C), 475 (Fe-Cp).

iv. PF_{90}
Aliphatic diamine 90% (1.692 mmol), Aromatic diamine 10% (0.188 mmol), Color: Dark brown. Yield: 76%. FT-IR (in cm^{-1}): 3410.3 (N–H), 3135 (Ar–H), 2920(CH_2), 1652.6 (C=O), 1535(N–H), 1216 (C–N), 511.7 (Fe-Cp).

2.3.2 Synthesis of PA Series

i. PA_0
Aliphatic diamine 0%, Aromatic diamine 100% (1.88 mmol), Color: Brown. Yield: 89%. FT-IR (in cm^{-1}): 3370.7 (N–H), 3095 (Ar–H), 1641.4 (C=O), 1531.9 (N–H), 1216.7(C–N), 1035.3 (C–O–C).

ii. PA_{50}
Aliphatic diamine 50% (0.94 mmol), Aromatic 50% (0.94 mmol), Color: dark brown. Yield: 88%. FT-IR (in cm^{-1}): 3270.5 (N–H), 3030 (Ar–H), 2970 (CH_2), 1628.1 (C=O), 1530.6 (N–H), 1210.7 (C–N), 1057.4 (C–O–C).

iii. PA_{70}
Aliphatic diamine 70% (1.316 mmol), Aromatic 30% (0.564 mmol), Color: Brown. Yield: 84%. FT-IR (in cm^{-1}): 3432.8–3317.8 (N–H), 3130–3050 (Ar–H), 2977.9 (CH_2), 1628.3 (C=O), 1540.6 (N–H), 1264.2 (C–N), 1034.9 (C–O–C).

iv. PA_{90}
Aliphatic diamine 90% (1.692 mmol), Aromatic diamine 10% (0.188 mmol), Color: Dark brown. Yield: 92%. FT-IR (in cm^{-1}): 3399.3 (N–H), 3134.6 (Ar–H), 2969.1 (CH_2), 1635.8 (C=O), 1536.7(N–H), 1262.4 (C–N).

2.3.3 Synthesis of PT Series

i PT_0
Aliphatic diamine 0%, Aromatic diamine 100% (1.88 mmol), Color: White. Yield: 87%. FT-IR (in cm^{-1}): 3275.3 (N–H), 3115–3048 (Ar–H), 2925–2869 (CH_2), 1641.2 (C=O), 1529 (N–H), 1318 (C–N), 1098.9 (C–O–C).

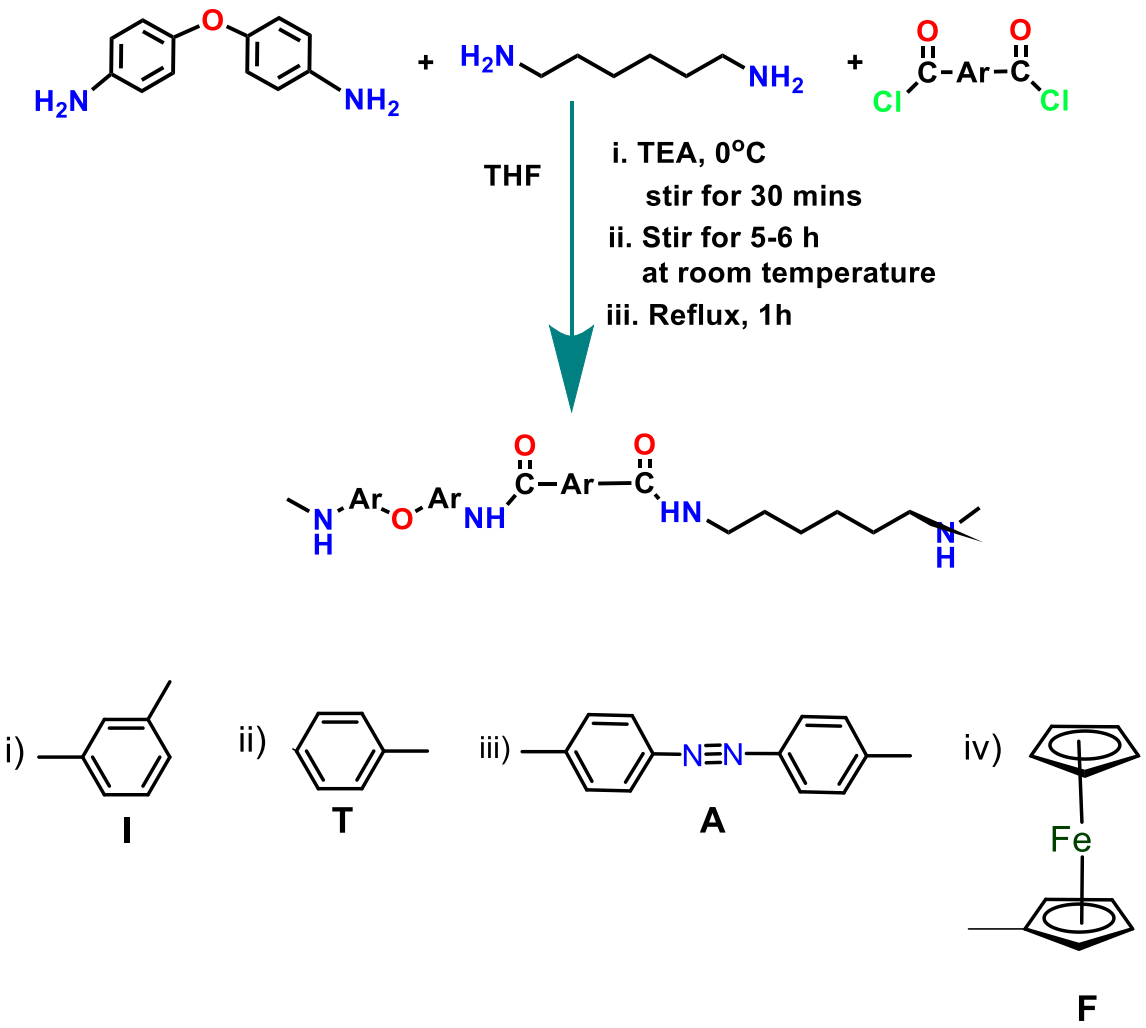

Scheme 2 Synthesis of organic and ferrocene-based polyamides

ii PT_{50}
Aliphatic diamine 50% (0.94 mmol), Aromatic 50% (0.94 mmol), Color: White. Yield: 82%. FT-IR (in cm^{-1}): 3299.4 (N–H), 3115–3052 (Ar–H), 1641.3 (C=O), 1543.3 (N–H), 1217.4 (C–N), 1100.9 (C–O–C).

iii PT_{70}
Aliphatic diamine 70% (1.316 mmol), Aromatic 30% (0.564 mmol), Color: White. Yield: 87%. FT-IR (in cm^{-1}): 3307 (N–H), 3115–3048 (Ar–H), 2936–2860 (CH_2), 1622.1 (C=O), 1538.2 (N–H), 1224 (C–N), 1091.9 (C–O–C).

iv PT_{90}
Aliphatic diamine 90% (1.692 mmol), Aromatic diamine 10% (0.188 mmol), Color: White. Yield 86%. FT-IR (in cm^{-1}): 3305.7 (N–H), 2969.8 (CH_2), 1640.9 (C=O), 1526.8 (N–H), 1217 (C–N).

2.3.4 Synthesis of PI Series

i PI_0
Aliphatic diamine 0%, Aromatic diamine 100% (1.88 mmol), Color: White. Yield: 92%. FT-IR (in cm^{-1}): 3259 (N–H), 3025 (Ar–H), 1647.7 (C=O), 1525.3 (N–H), 1237.9(C–N), 1063 (C–O–C).

ii PI_{50}
Aliphatic diamine 50% (0.94 mmol), Aromatic 50% (0.94 mmol), Color: White. Yield: 81%. FT-IR (in cm^{-1}): 3412.7–3276.3 (N–H), 3130–3052 (Ar–H), 2938.1 (CH_2), 1646.3 (C=O), 1525.7(N–H), 1238(C–N), 1102.7 (C–O–C).

iii PI_{70}
Aliphatic diamine 70% (1.316 mmol), Aromatic 30% (0.564 mmol), Color: White. Yield: 87%. FT-IR (in cm^{-1}): 3269.3 (N–H), 3160(Ar–H), 2968–2838.1 (CH_2),

1646.8 (C=O), 1540.6 (N–H), 1324.4 (C–N), 1106.0 (C–O–C).

iv PI_{90}

Aliphatic diamine 90% (1.692 mmol), Aromatic diamine 10% (0.188 mmol), Color: White. Yield: 89%. FT-IR (in cm^{-1}): 3289.8 (N–H), 3080 (Ar–H), 2943–2856.4 (CH_2), 1624.3 (C=O), 1539.0 (N–H), 1286.2 (C–N), 1152.6 (C–O–C).

2.4 Characterization

Melt-temp, Mitamura Riken Kogyo Inc, Tokyo, Japan, was employed to take the melting temperatures of synthesized monomers using open capillary tubes. The samples in solid state were subjected for analysis of functional groups by FT-IR instrument, Nicolet 6700, Thermo scientific company, USA using direct sample by ATR mode. Mettler Toledo Perkin Models DSC-823 was used to obtain the DSC curves of polymer samples at a heating rate of 10 °C/min in nitrogen atmosphere ranging the temperature from room temperature to 600 °C and using sapphire as an internal standard. Thermogravimetric analysis of polymers was performed on a Perkin-Elmer instrument TGA7 thermobalance. Samples were heated at rate of 10 °C/min under nitrogen atmosphere from room temperature to 900 °C. Polymer samples were analyzed by WAXRD using Philips 3040/60 X Pert PRO Diffractometer provided with a Cu-K_α radiation source. Surface morphology was analyzed by SEM using a JOEL JSM-6460 instrument. Samples were made conducting by applying gold-coated tapes and were mounted on an Al stub under vacuum to check the changes in surface morphology with change in composition of terpolymers. Viscometric measurements of polymers were done at room temperature in DMSO using U-tube Ubbelohde's viscometer with 20 mL capacity. The data thus collected was used to obtain relative viscosity (η_{rel}), specific viscosity (η_{sp}), reduced viscosity (η_{red}) and inherent viscosity (η_{inh}).

3 Results and Discussion

Low temperature solution polycondensation route was adopted for the polymerization of diamines and diacid chlorides under inert conditions in the solvent, THF [17, 18]. The reaction is exothermic, thus, initially; the temperature of the reaction mixture was maintained at 0 °C using ice bath to avoid the side reaction of the highly reactive acyl groups. It is well understood that THF is a better choice of solvent when moderate molecular weight polymers are required to be synthesized.

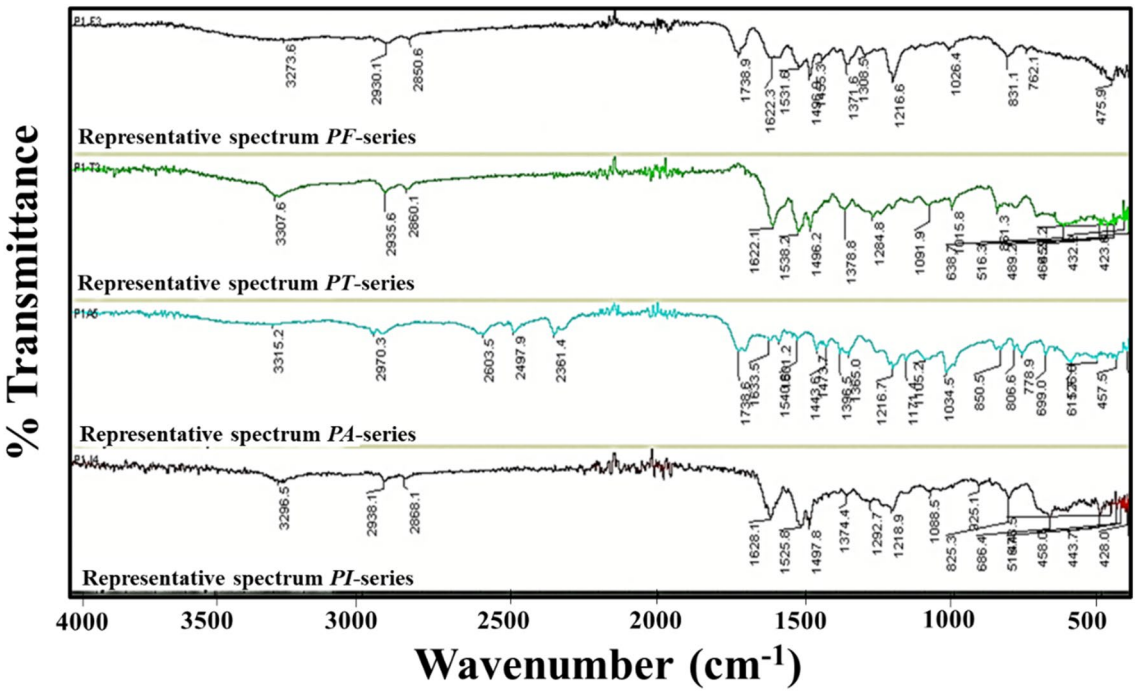

Fig. 1 Representative FT-IR spectra of Terpolyamides series PF, PT, PA, and PI, respectively

3.1 Structural Elucidation of Synthesized Terpolyamides

To elucidate the structural composition and functionalities of as-prepared polymers, FT-IR spectra were obtained. The representative spectra of each series are shown in Fig. 1.

The FTIR spectra showed a prominent single characteristic band in the region 3440–3270 cm^{-1} which is indicative of secondary amide –N–H [19–21] showing the successful condensation of monomers. The second most projecting peak observed was around 1655–1625 cm^{-1} attributed to the stretching frequency of carbonyl of amide group. The lowering of stretching frequency can be attributed to conjugation as it extends the dipolar character of conjugated carbon to β-carbon also, thereby increasing the single bond character of carbonyl group. Another characteristic, but rather weak band associated with bending vibration of N–H bond was observed around 1560–1520 cm^{-1}[22–24]. Moreover, the peak for ether linkage of 4,4′-ODA appeared in the region 1106–1014 cm^{-1} whereas this band was altogether absent in aliphatic polyamides. The aromatic and aliphatic moieties are easily distinguished owing to the presence of their characteristic peaks in the FTIR spectra. Besides, ferrocene based- terpolyamides were marked by the presence of a sharp peak in the fingerprint region around 511–475 cm^{-1} indicating Fe-Cp ring's stretching vibrations. The slightly higher absorption frequencies of carbonyl functional group in case of isophthaloyl based terpolyamides than terepthaloyl grades was due to the hydrogen bonding of polyamides. It is known that the phenomenon is more extensive in case of more ordered polymer microstructures, as was observed in the case of terepthaloyl-based polymers. The same trend was expected in case of azo-based polymers as the monomer (*TADC*) is also para-functionalized. However, no appreciable increase in frequency was observed which might be due to the highly conjugated system present in azo-based monomer; thus, the expected increase in vibration frequency due to H-bonding was compensated due to conjugation in same functional group [25].

3.2 Solubility Behavior

Aromatic terpolyamides were found to be completely insoluble in common organic solvents like THF, DMF, DMAc and DMSO, however, they exhibit good solubility in H_2SO_4 (Table 1) [26]. Interestingly, a subsequent increase in the solubility was observed with the increase in the aliphatic spacers in the polymer chain. In addition, upon treatment with trifluoroacetic acid (TFAA), the insoluble aromatic macro chains were found to be soluble in all the organic solvents attributed to the promising role of trifluoroacetic acid in overcoming the H-bonding present among the chains.

Table 1 Qualitative solubility data of synthesized terpolyamides

Sample name	THF	DMF	DMSO	DMAc	H_2SO_4	TFAA + any organic solvent
PF_0	−−	−−	−−	−−	++	++
PF_1	−−	−−	+−	−−	++	++
PF_2	−−	−−	+−	−−	++	++
PF_3	−−	+−	++	+−	++	++
PF_4	−−	+−	++	+−	++	++
PF_6	+−	++	++	+−	++	++
PA_0	−−	−−	−−	−−	++	++
PA_1	−−	−−	−−	−−	++	++
PA_3	−−	−−	−−	−−	++	++
PA_6	−−	+−	++	++	++	++
PT_0	−−	−−	−−	−−	++	++
PT_1	−−	−−	−−	−−	++	++
PT_3	−−	−−	−−	−−	++	++
PT_6	−−	+ −	++	++	++	++
PI_0	−−	−−	+−	−−	++	++
PI_1	−−	+−	+−	+−	++	++
PI_3	−−	+−	++	+−	++	++
PI_6	−−	++	++	++	++	++

(−− = insoluble, +− = partially soluble, ++ = soluble)

3.3 Thermal Analysis

Thermal analysis (TGA and DSC) was carried out at the heating rate of 10 °C/min in nitrogen atmosphere. The following parameters were determined to estimate the thermal stability of polymers were initial temperature (T_i) at which weight loss started, temperature at 50% weight loss (T_h), final temperature (T_f) at which maximum weight loss occurred, char residue (CR) at the end of experiment at (T_f) and the limiting oxygen index (LOI) values, as shown in Table 2. The stability of aliphatic repeating units was expected to be less as compared to the aromatic repeating units owing to the resonance stabilized aromatic moieties which required additional thermal energy to undergo degradation as compared to the aliphatic C–H bond with the reduced dissociation energy.

From Table 2, the thermal data revealed that the excellent thermal stability of all four series was associated with ferrocene-based terpolyamides. This can be attributed to the presence of a metal atom in the polymer architecture which imparted additional strength to the polymer chains [27]. The terephthaloyl-based terpolyamides also showed better thermal stability due to their highly ordered and consistently stacked polymer chains because of the para-catenation of the monomers. Additionally, glass transition temperatures were quite in agreement with values reported in literature [28]. The subsequent addition of flexible methylene spacer was expected to decrease the glass transition temperature, but the decrease was not observed in a regular fashion instead a general decreasing trend was seen as depicted by Fig. 2. Char residue which was left at final degradation temperature was also indicative of thermal stability of polymer [29]. Noteworthy, char residues were found to be higher for ferrocene-based terpolymers.

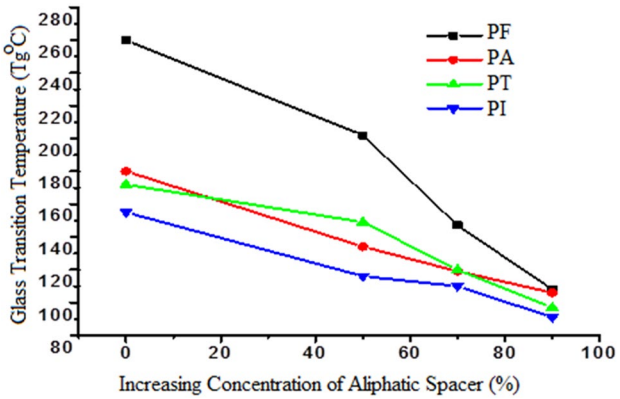

Fig. 2 Variation in *Tg* with increasing concentration of aliphatic spacer

Moving forward, flame retarding behavior of synthesized terpolyamides was estimated by determining the limiting oxygen index (LOI) values which can be estimated from the char residue. Greater the char residue, higher would be the LOI values and more would be the flame retarding behavior. It is known that the polymers having LOI values greater than 21 are flame retarding materials whereas the polymers having LOI values higher than 33 are known to be self-extinguishing polymers [30]. LOI values can be found by applying the Van Krevelen-Hoftyzer equation (Eq. 1) [31].

$$\mathrm{LOI} = 17.5 + 0.4\mathrm{CR} \quad (1)$$

The flame retarding behaviors were found to be best in case of ferrocene-based terpolymers as compared to the rest

Table 2 Thermal analysis data of synthesized terpolyamides

Polymer sample	T_g (°C)	T_i (°C)	T_h (°C)	T_f (°C)	Char residue (%)	LOI (%)
PF_0	260	310	525	720	39.12	33.15
PF_1	202	250	460	690	32.31	30.42
PF_3	147	227	428	572	26.68	28.17
PF_6	108	185	357	527	12.68	22.57
PA_0	180	230	430	582	38.16	32.40
PA_1	134	189	383	495	25.31	27.60
PA_3	119	160	347	485	19.40	25.30
PA_6	106	153	333	440	7.10	20.34
PT_0	172	300	564	670	12.10	22.34
PT_1	149	280	508	658	7.90	20.66
PT_3	120	248	478	640	4.43	19.27
PT_6	97	213	337	485	2.70	18.58
PI_0	155	208	460	572	22.20	26.38
PI_1	116	198	428	527	5.80	19.82
PI_3	110	182	357	478	5.20	19.58
PI_6	91	150	288	395	1.45	18.08

of analogues, signifying the beneficial role of iron atom which is left in the char in form of iron oxide and is resistant to further degradation.

3.4 WAXRD Analysis

Surface morphology of terpolyamides (whether crystalline or amorphous) was determined by wide angle X-Ray diffraction. Diffraction patterns were obtained at room temperature in the region 2θ = 15–30°, which is typical of polymers. From the diffractograms, Fig. 3, it is evident that the ferrocene-based terpolyamides were amorphous in nature whereas the other polymers showed crystalline morphology. Among the organic terpolyamides, terephthaloyl-based polymers exhibited more crystalline nature [32]. This depicted that the para-catenation of the monomers led to the closed and ordered packing of polymer chains.

The bulky ferrocene moieties caused disruption in polymer chains thereby preventing the ordered arrangement of polymer microstructure, thus, were amorphous in nature [33, 34]. By increasing the aliphatic content, polymers showed progression from semi-crystalline to amorphous behaviors. This is because the chain packing was disorganized due to increase in flexible linkage which subsequently leads to decrease in stiff aromatic linkages in polymer chains [35]. A broad background, with few minor peaks, was observed in case of ferrocene-based terpolyamides revealing the amorphous nature [33]. All terpolyamides had crystalline structure and showed resistance towards common organic solvents which is in agreement with the general trend reported that increasing the crystallinity tends to decrease the solubility. Additionally, the amorphous nature of these DMSO soluble terpolyamides could be due to the presence of bulky ferrocene moiety

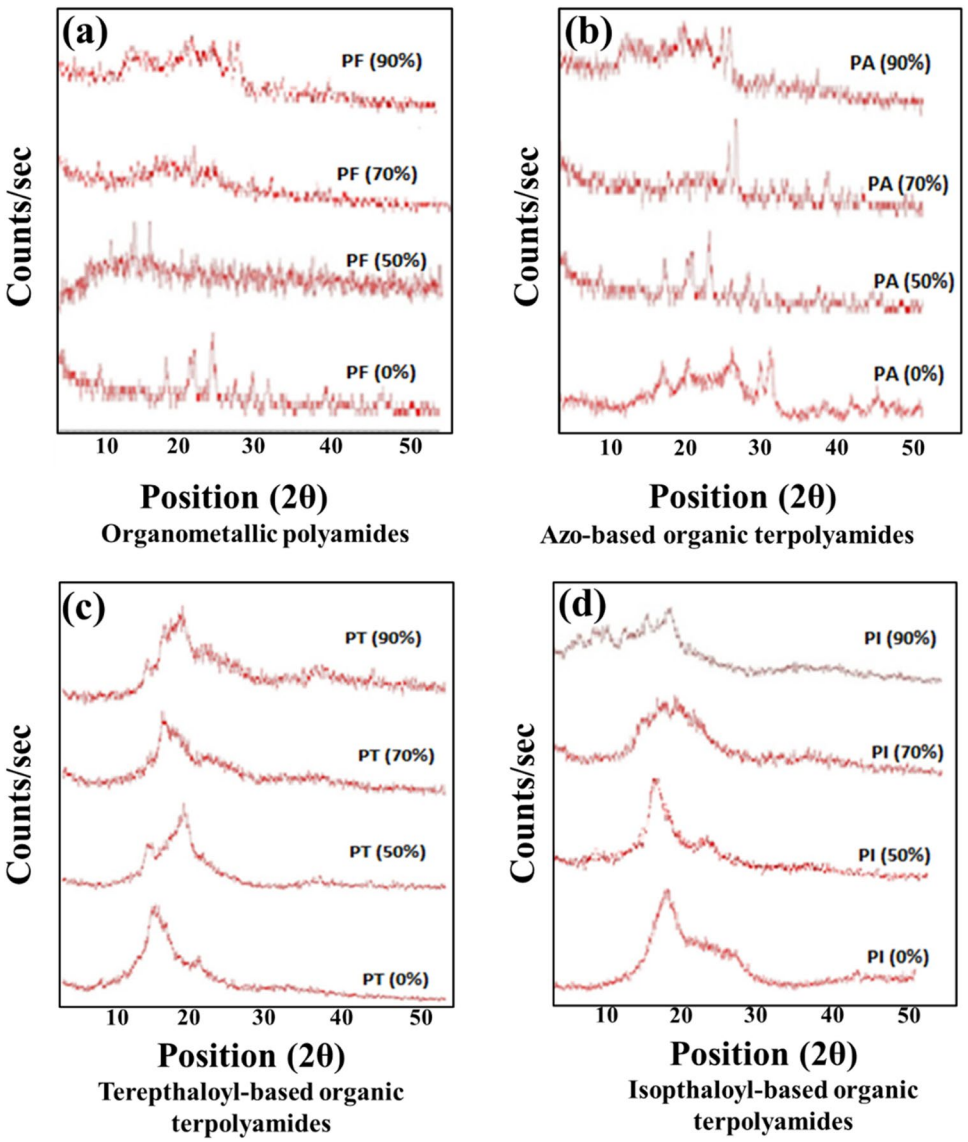

Fig. 3 WAXRD patterns for **a** Organometallic polyamides, **b** Azo-based organic terpolyamides, **c** Terepthaloyl-based organic terpolyamides and **d** Isopthaloyl-based organic terpolyamides polymers

that makes them incapable of getting a regular ordered structure.

3.5 Viscometric Analysis

The viscosity data was obtained using polymer solutions in DMSO by U-tube Ubbelohd's viscometer at room temperature. The inherent viscosities of all polymers ranged from 1.8052–1.6274 dl/g showing that polymers solutions were quite viscous which is indicative of the fact that polymers formed have reasonable molecular weights [36–38].

From the data, it is revealed that the ferrocene-based polymers have highest ranges of viscosity and with increasing concentration of flexible methylene linkage, a decreasing trend in viscosity was observed for all synthesized polymers. The data plots (Fig. 4) showed that with the decrease in the concentration of aromatic diamine, viscosity was decreased. This could be attributed to free volume created in between the polymer chains due to introduction of flexible methylene linkage, thereby decreasing the viscosity of polymers. The data further highlighted that the strong H-bonding operative in polymer structural design sourced the unusually high viscous flow of polyamide solutions as compared to other classes of polymers.

3.6 SEM Analysis

From the surface morphological analysis of synthesized terpolyamides (Fig. 5), it is evident that organic terpolyamides had surface features resembling that of sphere-shaped particles whereas ferrocene-based terpolyamides showed sponge like appearance [39–44]. The introduction of an aliphatic diamine along with an aromatic diamine showed marked effect on surface topology of polymers, which was clearly depicted in micrographs [45, 46]. Progression from low percentage of flexible spacer to higher percentage had rendered a marked effect by making surface more compact and undistinguished. Henceforth, by increasing the aliphatic content of terpolyamides, surfaces can be made smoother and lubricating. Also, porosity of polymer can be decreased, thereby making it fit for use in various fields where smooth, lubricating and compact surface coatings and materials are required. Conclusively,

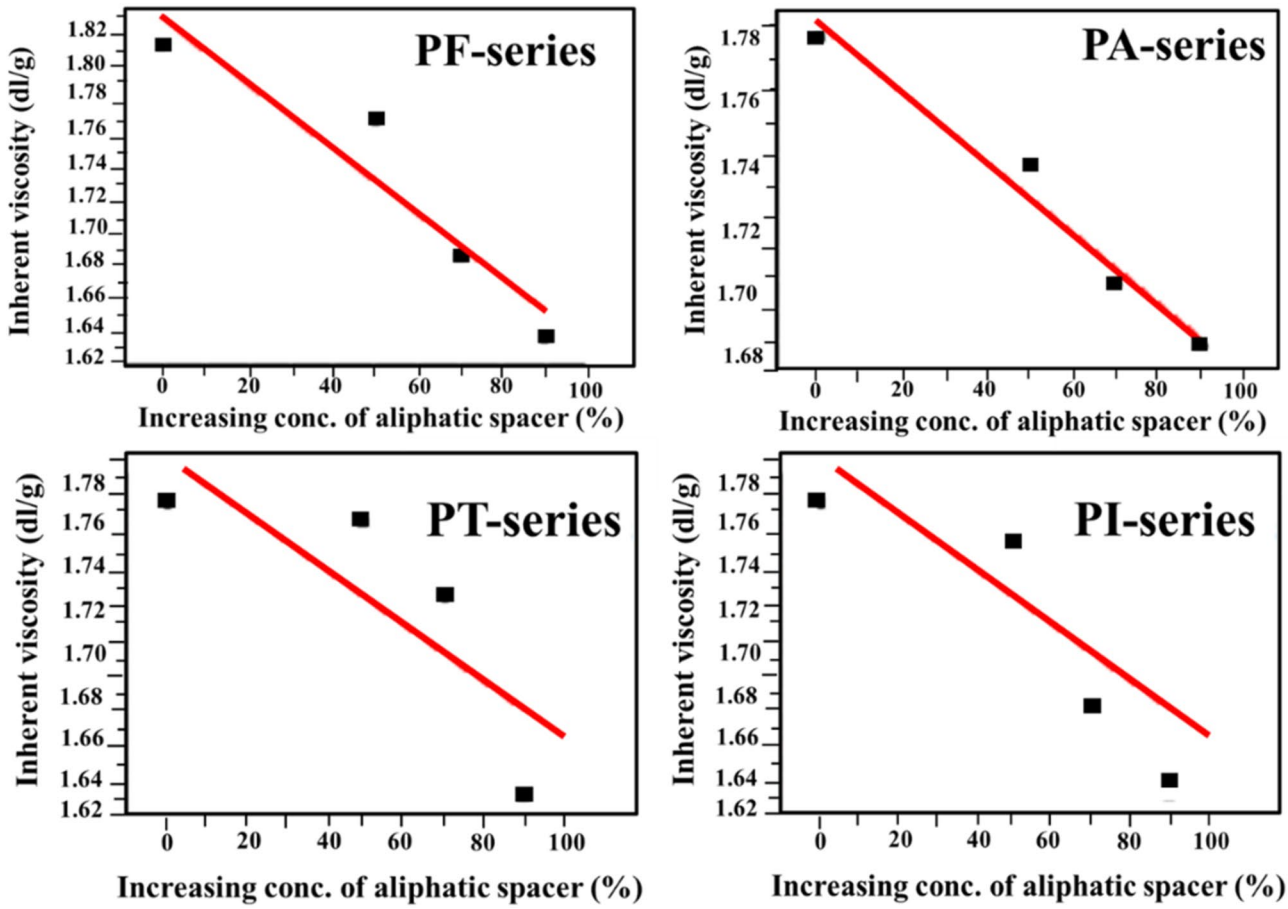

Fig. 4 Viscosity composition plots of organometallic and organic terpolyamides

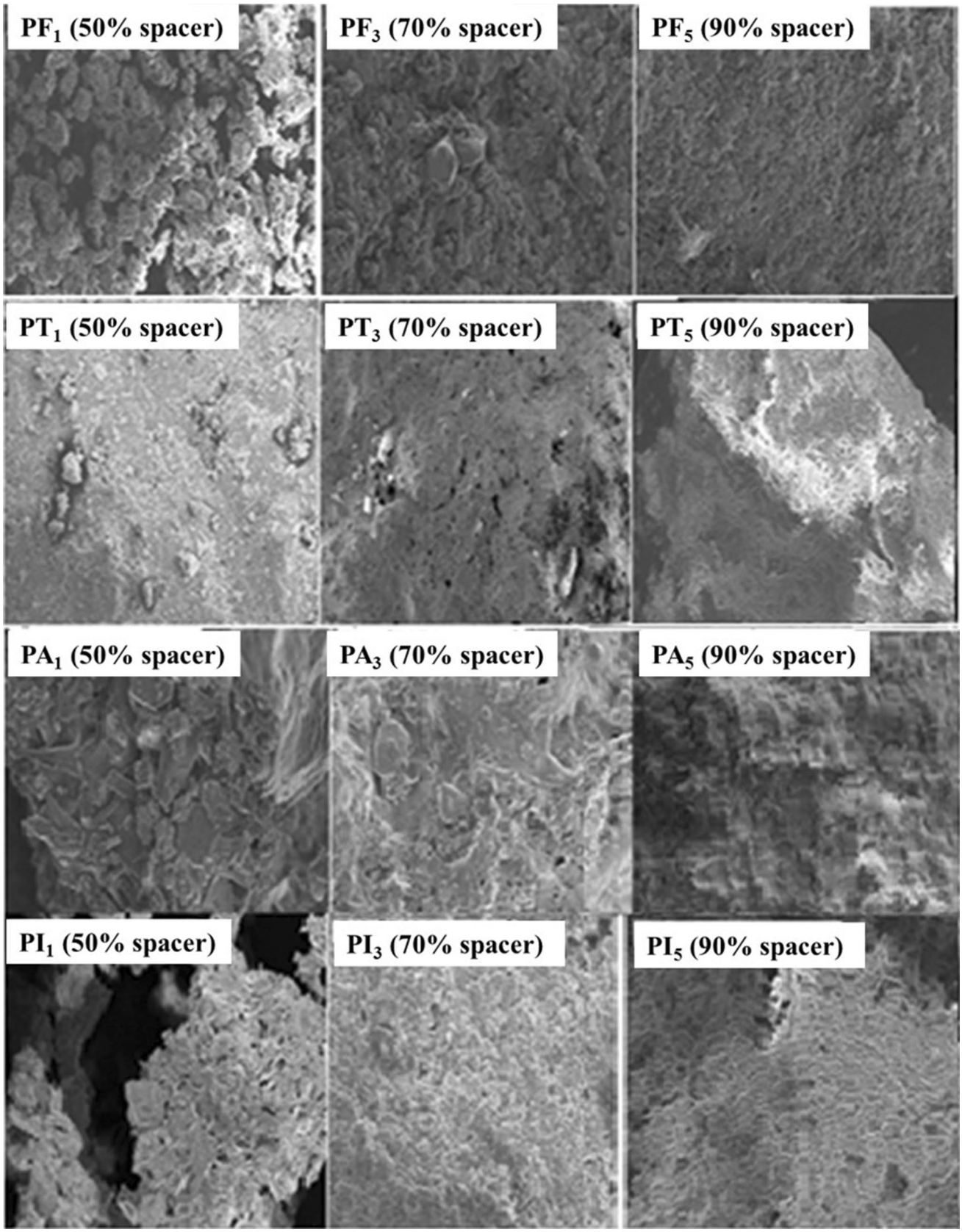

Fig. 5 Scanning electron micrographs of terpolyamides

the diverse morphology of all grades showed that we have successfully altered composition of aliphatic diamine in terpolyamides [47].

4 Conclusions

In the light of the experimental results, following conclusions have been drawn:

1. In this study, four distinct series of aromatic and aliphatic terpolyamides were synthesized via solution phase polycondensation of 4,4′-oxydianiline and hexamethylenediamine (HMDA) with different diacids chlorides (isophthalyol dichloride, terepthalyol dichloride, 1, 1′-ferrocene dicarboxylic acid chloride and trans-azobenzene-4, 4′-dicarbonyl chloride).
2. Polymers containing aliphatic and aromatic spacers were characterized successfully in order to investigate the effect of increase in concentration of methylene spacer (HMDA) and to explore the subsequent changes in various physico-chemical properties.
3. The objective was achieved by attaining remarkable improvement in the physico-chemical properties of the synthesized polymers. An obvious difference in morphology and solubility has been observed by changing the ratio of segments in the polymer chain. Moreover, the estimated inherent viscosities of polymers lies in the range of 1.8052–1.6274 dl/g, evidencing the reasonably moderate molecular weights.
4. The ferrocene based aromatic polymers exhibit higher thermal stability (T_g 260 °C, T_i 310 °C, T_h 525 °C, T_f 720 °C, for PF_0), and also found to exhibit best flame retarding behavior [limiting oxygen index (LOI) value for $PF_0$is LOI 33.15%].
5. Therefore, the present study opens new gateways for designing the high-performing materials by varying the ratio of sequences and processable materials which consequently leads to desired physico-chemical attributes and tailored thermal and surface properties to be used for smooth, lubricating, and compact surface coatings and various other potential applications.

Acknowledgements The authors would like to thank University Research Fund, Quaid-i-Azam University, Islamabad, for the financial support of this project.

Author Contributions TK: Conceptualization, Methodology, Experimentation, Data Acquisition, Writing original draft—Review & Editing. ZA: Writing, Review and Editing, Supervision, Funding acquisition. AG: Review and Editing. ASB: Review and Editing, AR: Writing, Review and Editing, Methodology, Supervision.

References

1. T.W. Lee, S. Lee, S.M. Park, D. Lee, Mechanical, thermomechanical, and local anisotropy analyses of long basalt fiber reinforced polyamide 6 composites. Compos. Struct. **222**, 110917 (2019)
2. Y. Gao, W. Zhang, D. Li, X. Lin, X. Qiao, H. Niu et al., Novel polyamides containing asymmetric diamine designed and synthesized towards electrochromic and resistance memory device. Synth. Met. **274**, 116732 (2021)
3. S. Rahmatkhah, S. Mehdipour-Ataei, Synthesis and characterization of novel poly (urethane-amide)s with enhanced thermal stability. Int. J. Polym. Anal. Charact. **27**, 87–98 (2022)
4. S. Xia, Y. Gao, P. Wang, Y. Ma, D. Zhu, H. Niu et al., Three dimensional fluorene-based polyamides facile to transfer ion designed for near-infrared electrochromic application and detection for explosive. Chem. Eng. J. **437**, 135108 (2022)
5. F. Dumur, Recent advances on ferrocene-based photoinitiating systems. Eur. Polym. J. **147**, 110328 (2021)
6. B.U. Amin, H. Yu, L. Wang, S. Fahad, A. Nazir, F. Haq et al., Synthesis and anti-migration studies of ferrocene-based amides as burning rate catalysts. J. Inorg. Organomet. **31**, 2511–2520 (2021)
7. Y. Yang, Z. Lai, Ferrocene-based porous organic polymer for photodegradation of methylene blue and high iodine capture. Microporous Mesoporous Mater. **316**, 110929 (2021)
8. T.L. Bennett, L.A. Wilkinson, J.M. Lok, R.C. O'Toole, N.J. Long, Synthesis, electrochemistry, and optical properties of highly conjugated alkynyl-ferrocenes and-biferrocenes. Organometallics **40**, 1156–1162 (2021)
9. R.K. Mishra, T. Eren, D.Y. Wang, Inorganic polymers as flame-retardant materials, in *Smart Inorganic Polymers: Synthesis, Properties, and Emerging Applications in Materials and Life Sciences*. (Wiley, New York, 2019), pp. 197–241
10. Z. Zhang, M.H. Litt, L. Zhu, Achieving relaxor ferroelectric-like behavior in nylon random copolymers and terpolymers. Macromolecules **50**, 9360–9372 (2017)
11. S. Yilmaz, O. Gul, T. Yilmaz, Effect of chain extender and terpolymers on tensile and fracture properties of polyamide 6. Polymer **65**, 63–71 (2015)
12. A. Datta Sarma, H.R. Padmanathan, S. Saha, S. Shankar Banerjee, A.K. Bhowmick, Design and properties of a series of high-temperature thermoplastic elastomeric blends from polyamides and functionalized rubbers. J. Appl. Polym. Sci. **134**, 45353 (2017)
13. Y. Luo, S. Wang, X. Du, Z. Du, X. Cheng, H. Wang, Durable flame retardant and water repellent cotton fabric based on synergistic effect of ferrocene and DOPO. Cellulose **28**, 1809–1826 (2021)
14. M. Rosenblum, R.B. Woodward, The structure and chemistry of ferrocene. III. Evidence pertaining to the ring rotational barrier. J. Am. Chem. Soc. **80**, 5443–5449 (1958)
15. F.W. Knobloch, W.H. Rauscher, Condensation polymers of ferrocene derivatives. J. Polym. Sci. **54**, 651–656 (1961)
16. M.S.U. Khan, A. Nigar, M.A. Bashir, Z. Akhter, A new ferrocene-containing polyamide prepared from an improved synthesis of 1, 1′-ferrocene dicarbonyl chloride and ferrocene-based diamine. Synth. Commun. **37**, 473–482 (2007)
17. J.A. Reglero Ruiz, M. Trigo-López, F.C. García, J.M. García, Functional aromatic polyamides. Polymers **9**, 414 (2017)
18. K.I. Aly, A.H. Moustafa, E.K. Ahmed, H.M. Abd El-lateef, M.G. Mohamed, S.M. Mohamed et al., New polymer syntheses part 60: a facile synthetic route to polyamides based on thieno [2, 3-b] thiophene and their corrosion inhibition behavior. Chin. J. Polym. Sci. **36**, 835–847 (2018)
19. B. Jović, M. Panić, N. Radnović, K. Živojević, M. Mladenović, V. Crnojević et al., Investigation of the surface interactions of

selected amides with mesoporous silica using FTIR spectroscopy and hyperspectral imaging. J. Mol. Struct. **1219**, 128562 (2020)
20. A. Rehman, S.J. Park, Preparation and characterization of polyamides and nitrogen-doped carbons for enhanced CO_2 capture. Bull. Korean Chem. Soc. **38**, 1285–1292 (2017)
21. M. Čolović, J. Vasiljević, Ž Štirn, N.Č Korošin, M. Šobak, B. Simončič et al., New sustainable flame retardant DOPO-NH-functionalized polyamide 6 and filament yarn. Chem. Eng. J. **426**, 130760 (2021)
22. C. Zhou, S. Qi, P. Zhu, Y. Zhao, Y. Xu, X. Dong et al., The methylene infrared vibration and dielectric behavior monitored by amide group arrangement for long chain polyamides. Polymer **190**, 122231 (2020)
23. M. Kaur, R. Kaur, K.S. Samra, Luminescent behavior of semiconductor doped polyamide. AIP Conf. Proc. **1860**, 020004 (2017)
24. A.S. Patil, M. Medhi, N.V. Sadavarte, P.P. Wadgaonkar, N.N. Maldar, Synthesis and characterization of novel aromatic–aliphatic polyamides from bis-[(4-aminobenzyl)-4-benzamide] ether. Mater. Sci. Eng. B **168**, 111–116 (2010)
25. Y. Liu, S. Jiang, W. Yan, J. Qin, M. He, S. Qin et al., Enhanced mechanical and thermal properties of polyamide 6/p (N-(4-F-phenylmaleimide)–alt-styrene) composites based on interfacial complexation inducing crystal transformation. Polymer **214**, 123237 (2021)
26. Z. Yu, R. Deng, G. Rao, Y. Lu, Y. Wei, C. Fu et al., Synthesis and characterization of highly soluble wholly aromatic polyamides containing both furanyl and phenyl units. J. Polym. Sci. **58**, 2140–2150 (2020)
27. Y. Vidavsky, M.R. Buche, Z.M. Sparrow, X. Zhang, S.J. Yang, R.A. DiStasio Jr. et al., Tuning the mechanical properties of metallopolymers via ligand interactions: a combined experimental and theoretical study. Macromolecules **53**, 2021–2030 (2020)
28. R. Xie, A.R. Weisen, Y. Lee, M.A. Aplan, A.M. Fenton, A.E. Masucci et al., Glass transition temperature from the chemical structure of conjugated polymers. Nat. Commun. **11**, 1–8 (2020)
29. N. Mandlekar, A. Cayla, F. Rault, S. Giraud, F. Salaun, G. Malucelli et al., Thermal stability and fire retardant properties of polyamide 11 microcomposites containing different lignins Ind. Eng. Chem. Res. **56**, 13704–13714 (2017)
30. E.M. Mansour, A.A. Iskander, H.H. Hassan, Synthesis, thermal and optical properties of nanosized polyamides containing N-phenyl-and N-naphthyl-s-triazine rings: structure-properties correlation. J. Macromol. Sci. A **54**, 105–117 (2017)
31. D.W. Van Krevelen, Some basic aspects of flame resistance of polymeric materials. Polymer **16**, 615–620 (1975)
32. Z. Cheng, D. Liao, X. Hu, W. Li, C. Xie, H. Zhang et al., Synergistic fire retardant effect between expandable graphite and ferrocene-based non-phosphorus polymer on polypropylene. Polym. Degrad. Stab. **178**, 109201 (2020)
33. M.S.U. Khan, Z. Akhter, T. Naz, A.S. Bhatti, H.M. Siddiqi, M. Siddiq et al., Study on the preparation and properties of novel block copolymeric materials based on structurally modified organometallic as well as organic polyamides and polydimethylsiloxane. Polym. Int. **62**, 319–334 (2013)
34. G. Nazir, A. Rehman, S.J. Park, Self-activated, urea modified microporous carbon cryogels for high-performance CO_2 capture and separation. Carbon **192**, 14–29 (2022)
35. A. Rehman, S.J. Park, Facile synthesis of nitrogen-enriched microporous carbons derived from imine and benzimidazole-linked polymeric framework for efficient CO_2 adsorption. J. CO2 Util. **21**, 503–512 (2017)
36. J. Rezania, M. Hayatipour, A. Shockravi, M. Ehsani, V. Vatanpour, Synthesis and characterization of soluble aromatic polyamides containing double sulfide bond and thiazole ring. Polym. Bull. **76**, 1547–1556 (2019)
37. J.M. Pérez-Francisco, W. Herrera-Kao, M.O. González-Díaz, M. Aguilar-Vega, J.L. Santiago-García, Assessment of random aromatic co-polyamides containing two different bulky pendant groups. J. Appl. Polym. Sci. **135**, 45884 (2018)
38. S. Russo, A. Mariani, V.N. Ignatov, I.I. Ponomarev, High-molecular-weight aromatic polyamides by direct polycondensation. Macromolecules **26**, 4984–4985 (1993)
39. Y. Alsaid, S. Wu, D. Wu, Y. Du, L. Shi, R. Khodambashi et al., Tunable sponge-like hierarchically porous hydrogels with simultaneously enhanced diffusivity and mechanical properties. Adv. Mater. **33**, 2008235 (2021)
40. G. Nazir, A. Rehman, S.J. Park, Sustainable N-doped hierarchical porous carbons as efficient CO_2 adsorbents and high-performance supercapacitor electrodes. J. CO2 Util. **42**, 101326 (2020)
41. B.Y. Guan, A. Kushima, L. Yu, S. Li, J. Li, X.W. Lou et al., Coordination polymers derived general synthesis of multishelled mixed metal-oxide particles for hybrid supercapacitors. Adv. Mater. **29**, 1605902 (2017)
42. G. Nazir, A. Rehman, S.J. Park, Valorization of shrimp shell biowaste for environmental remediation: Efficient contender for CO_2 adsorption and separation. J. Environ. Manage. **299**, 113661 (2021)
43. M. Zare, N. Parvin, M.P. Prabhakaran, J.A. Mohandesi, S. Ramakrishna, Highly porous 3D sponge-like shape memory polymer for tissue engineering application with remote actuation potential. Compos. Sci. Technol. **184**, 107874 (2019)
44. A. Rehman, G. Nazir, K.Y. Rhee, S.J. Park, A rational design of cellulose-based heteroatom-doped porous carbons: promising contenders for CO_2 adsorption and separation. Chem. Eng. J. **420**, 130421 (2021)
45. K.L. Meena, Ch.S. Vidyasagar, D.B. Karunakar, Mechanical and tribological properties of MgO/multiwalled carbon nanotube-reinforced zirconia-toughened alumina composites developed through spark plasma sintering and microwave sintering. J. Mater. Eng. Perform. **31**, 682–696 (2022)
46. K.L. Meena, D.B. Karunakar, Effect of ZrO_2 and MgO added in alumina on the physical and mechanical properties of spark plasma sintered nanocomposites. Int. J. Refract. Hard Met. **81**, 281–290 (2019)
47. A. Gul, Z. Akhter, A. Bhatti, M. Siddiq, A. Khan, H.M. Siddiqe et al., Synthesis, physicochemical studies and potential applications of high-molecular-weight ferrocene-based poly (azomethine) ester and its soluble terpolymers. J. Organomet. Chem. **719**, 41–53 (2012)